which, by definition [8], is

$$I_n(v) \equiv (-1)^{-n} J_n(jv). \tag{16}$$

For small arguments ($V<1$) [9]

$$I_{-n}(v) = I_n(v) = \frac{1}{n!}\left(\frac{v}{2}\right)^n. \tag{17}$$

Combining (14b), (16), and (17), using only the $n=-1$, $n=0$, and $n=+1$ terms of the summation in (14b), and using the equality

$$J_{-n}(v) = (-1)^n J_n(v) \tag{18}$$

results in

$$J_m(u+jv) \approx J_m(u) + \frac{jv}{2}\left[J_{m-1}(u) - J_{m+1}(u)\right] \tag{19a}$$

$$= J_m(u) + jvJ_m'(u). \tag{19b}$$

Equation (19b) is derived from (19a) by utilizing the recurrence relation [10]

$$J_{m-1}(u) - J_{m+1}(u) = 2J_m'(u). \tag{20}$$

$J_m'(u)$ is the derivative of $J_m(u)$ with respect to u. Similarly

$$N_m(u+jv) = N_m(u) + jvN_m'(u). \tag{21}$$

Using two additional recurrence relationships

$$J_0'(u) = -J_1(u) \tag{22a}$$

and

$$J_1'(u) = J_0(u) - \frac{1}{u}J_1(u) \tag{22b}$$

the resulting equations with the substitutions $u=\beta r$ and $v=-\alpha r$ are

$$J_0(kr) = J_0(\beta r) + j\alpha r J_1(\beta r) \tag{23a}$$

$$J_1(kr) = J_1(\beta r) - j\alpha r\left[J_0(\beta r) - \frac{J_1(\beta r)}{\beta r}\right]. \tag{23b}$$

For the Neumann functions

$$N_0(kr) = N_0(\beta r) + j\alpha r N_1(\beta r) \tag{23c}$$

$$N_1(kr) = N_1(\beta r) - j\alpha r\left[N_0(\beta r) - \frac{N_1(\beta r)}{\beta r}\right]. \tag{23d}$$

The final analysis equations for radial-line stubs with attenuation result from substituting (23a) through (23d), with the appropriate arguments, into (5) and the latter, in turn, into (4).

III. Recommendations for Stripline and Microstrip

For stripline, the dimension h in (4), (6), (12), and (13) should be replaced by the ground-plane spacing b.

For microstrip, it is recommended[1] that the relative dielectric constant ϵ_r should be replaced by an effective dielectric constant ϵ_{eff} calculated [11] for a microstrip of constant width w, where

$$w = (r_i + r_o)\sin\left(\frac{\theta}{2}\right). \tag{24}$$

A computer program has been written to test these equations and to compare the results with the lossless formulation of Vinding. For perfect conductors ($R_s = 0$), the results were identical. For finite values of surface resistance, the equations correctly calculated both the resistive and reactive portions of the input impedance.

[1]This approximation, while providing reasonably accurate results, is not the formulation for effective dielectric constant used in Super-Compact.

IV. Conclusion

New equations, useful for the accurate calculation of the complex input impedance of lossy, radial-line stubs, have been presented. This should lead to an improvement in the accuracy of the predicted performance of circuits which contain these elements.

Appendix

For completeness, the equations due to Vinding, using the notation of this paper, are included below.

$$Z_{\text{in}} = j\frac{Z_0(kr_i)h}{r_i}\frac{\cos[\theta(kr_i) - \psi(kr_o)]}{\sin[\psi(kr_i) - \psi(kr_o)]} \tag{A1}$$

$$Z_0(kr_i) = \frac{120\pi}{\sqrt{\epsilon_r}}\left[\frac{J_0^2(kr_i) + N_0^2(kr_i)}{J_1^2(kr_i) + N_1^2(kr_i)}\right]^{1/2} \tag{A2}$$

$$\theta(kr_i) = \tan^{-1}[N_0(kr_i)/J_0(kr_i)] \tag{A3}$$

$$\psi(kr_i) = \tan^{-1}[-J_1(kr_i)/N_1(kr_i)] \tag{A4}$$

$$\psi(kr_o) = \tan^{-1}[-J_1(kr_o)/N_1(kr_o)]. \tag{A5}$$

References

[1] N. Marcuvitz, "Radial transmission lines," in *Principles of Microwave Circuits*, C. G. Montgomery, R. H. Dicke, and E. M. Purcell, Eds., (Radiation Laboratory Series, Vol. 8). New York, NY: McGraw-Hill, 1947, pp. 240–282.

[2] S. Ramo and J. R. Whinnery, *Fields and Waves in Modern Radio*, Second Ed. New York, NY: Wiley, 1953, pp. 395–400.

[3] H. A. Atwater, "Microstrip reactive circuit elements," *IEEE Trans. Microwave Theory Tech.*, vol. MTT-31, pp. 488–491, June 1983.

[4] B. A. Syrett, "A broad-band element for microstrip bias or tuning circuits," *IEEE Trans. Microwave Theory Tech.*, vol. MTT-28, pp. 925–927, Aug. 1980.

[5] ——, "Broadband microstrip mixer design: The Butterfly mixer," Application Note Number 976, Hewlett-Packard Co., Palo Alto, CA, July 1980.

[6] J. P. Vinding, "Radial line stubs as elements in strip line circuits," *NEREM Rec.*, pp. 108–109, Nov. 1967.

[7] M. Abramowitz and I. E. Stegun, Eds., *Handbook of Mathematical Functions with Formulas, Graphs and Mathematical Tables*, (Applied Mathematics Series, Vol. 55). Washington, DC: U.S. Department of Commerce, National Bureau of Standards, 1964, pp. 363, eq. 9.1.75.

[8] ——, *Handbook of Mathematical Functions with Formulas, Graphs and Mathematical Tables*, pp. 375, eq. 9.6.3.

[9] ——, *Handbook of Mathematical Functions with Formulas, Graphs and Mathematical Tables*, pp. 375, eq. 9.6.6 and 9.6.7.

[10] ——, *Handbook of Mathematical Functions with Formulas, Graphs and Mathematical Tables*, pp. 361, eq. 9.1.27.

[11] S. L. March, "Microstrip packaging: Watch the last step," *Microwaves*, vol. 20, pp. 83–94, Dec. 1981.

Plot of Modal Field Distribution in Rectangular and Circular Waveguides

C. S. LEE, S. W. LEE, AND S. L. CHUANG

The earliest plots of modal field distribution in rectangular/circular waveguides were given by Southworth (1936) [1], Barrow (1936) [2], Schelkunoff (1937) [3], and Chu and Barrow (1937) [4].

Manuscript received August 9, 1984; revised October 30, 1984. This work was supported in part by NASA under Contract NAG3-475.

The authors are with the Electromagnetic Laboratory, University of Illinois, Urbana, IL 61801.

0018-9480/85/0300-0271$01.00 ©1985 IEEE

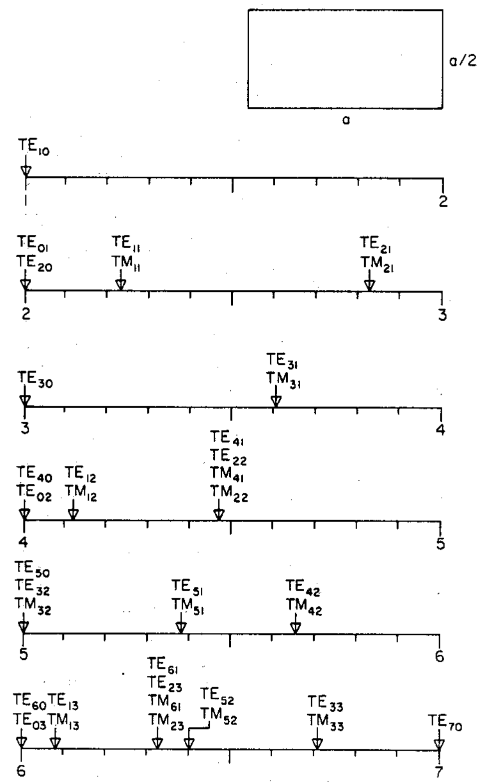

Fig. 1. Normalized modal cutoff frequencies for a 2:1 rectangular waveguide.

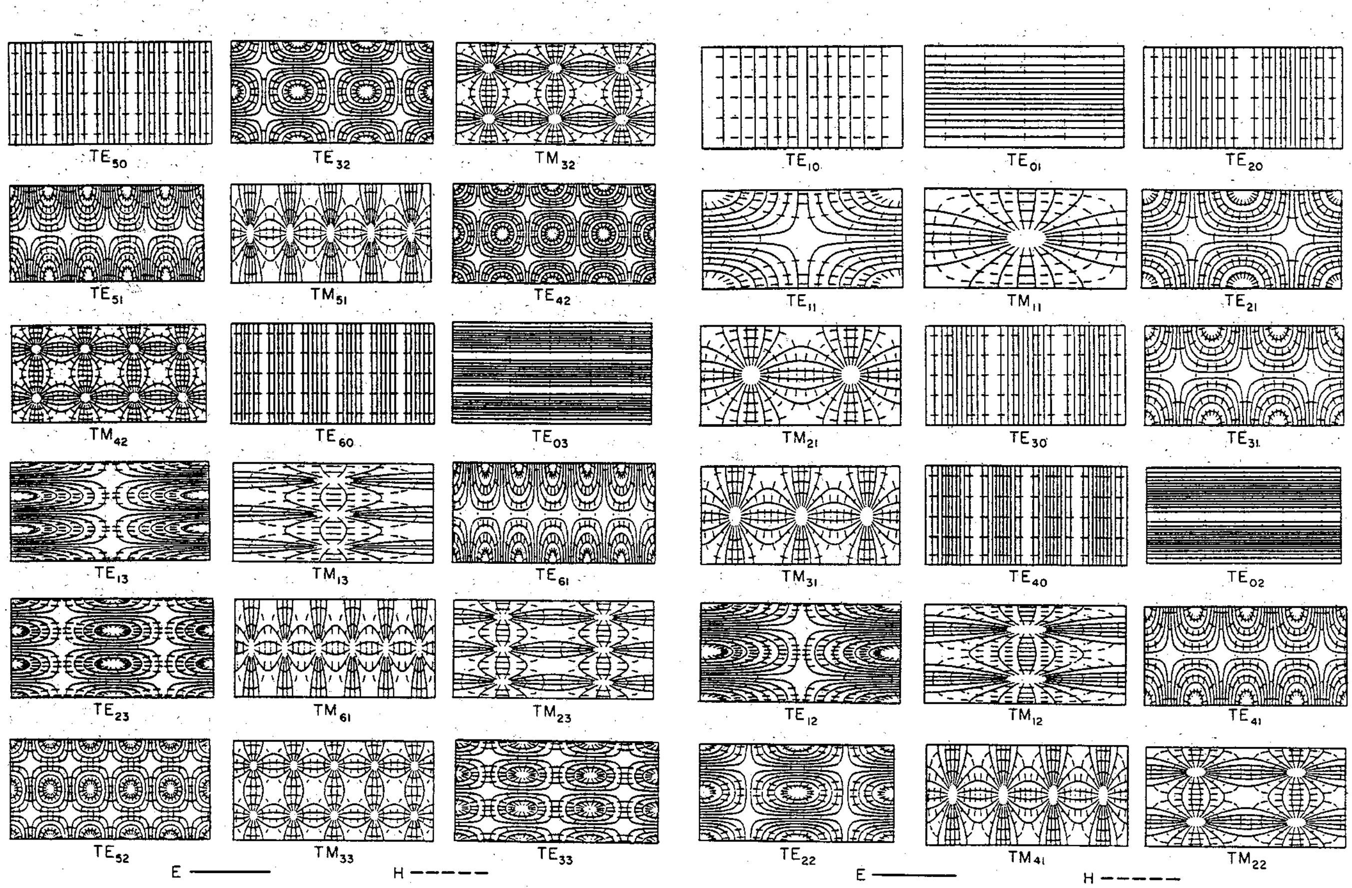

Fig. 2. Transverse modal field distribution for a 2:1 rectangular waveguide (first 36 modes).

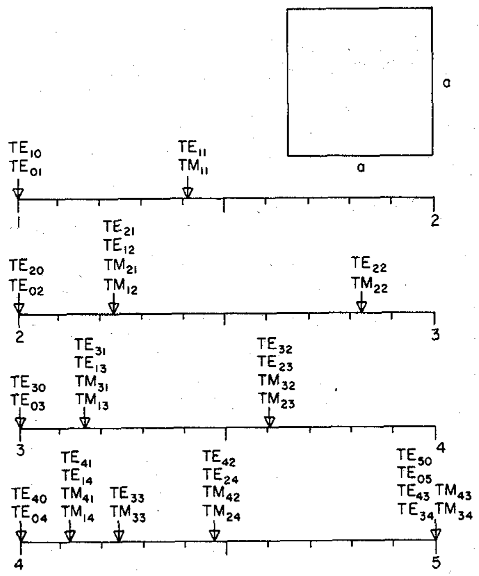

Fig. 3. Normalized modal cutoff frequencies for a square waveguide.

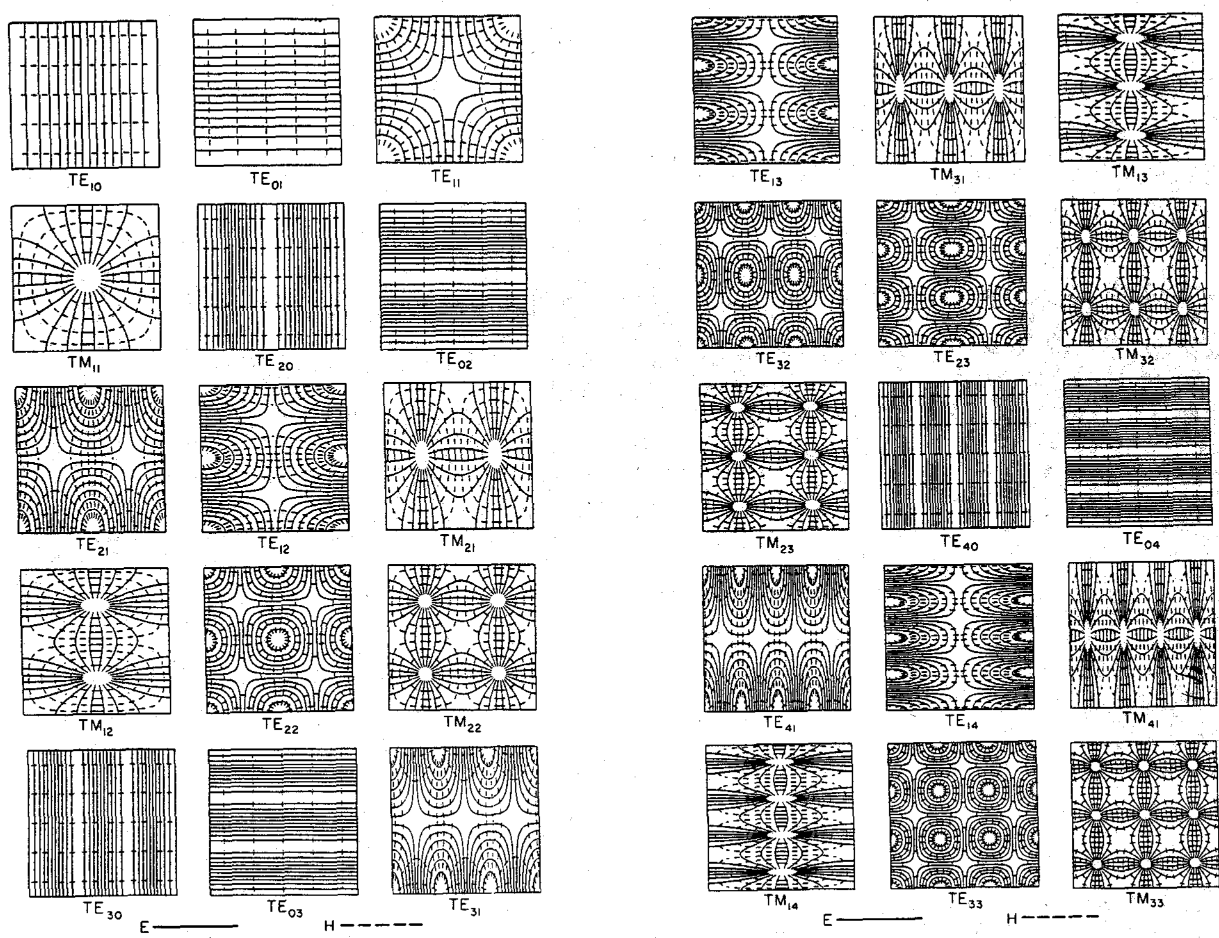

Fig. 4. Transverse modal field distribution for a square waveguide (first 30 modes).

Standard text and reference books present plots only for the first six or seven modes. In many applications, we are interested in plots for higher order modes. The purpose of this note is to present three relatively complete sets of plots, namely, a) plots for the first 36 modes in a 2:1 rectangular waveguide (Figs. 1 and 2), b) plots for the first 30 modes in a square waveguide (Figs. 3 and 4), c) plots for the first 30 modes in a circular waveguide (Figs. 5 and 6).

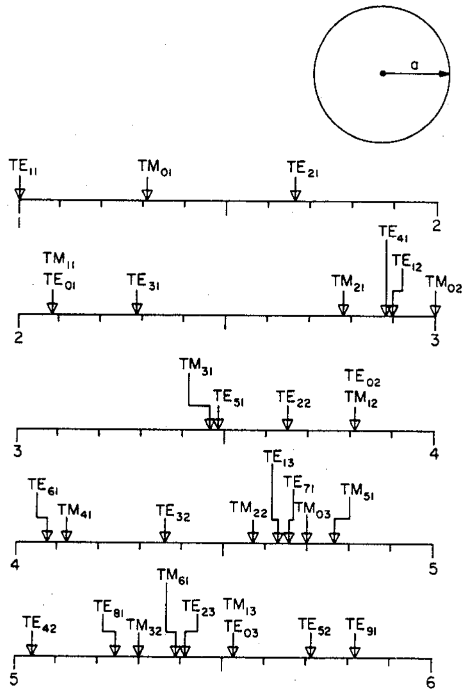

Fig. 5. Normalized modal cutoff frequencies for a circular waveguide.

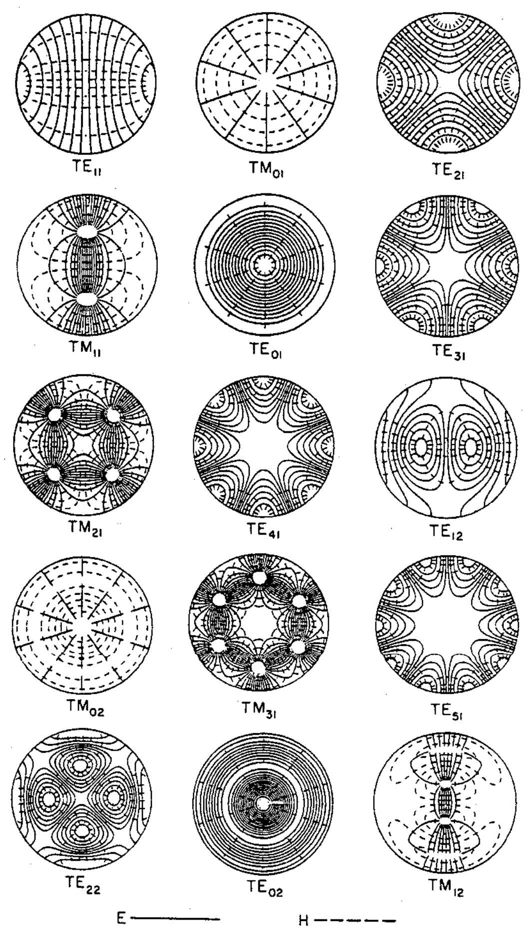

Fig. 6. Transverse modal field distribution for a circular waveguide (first 30 modes).

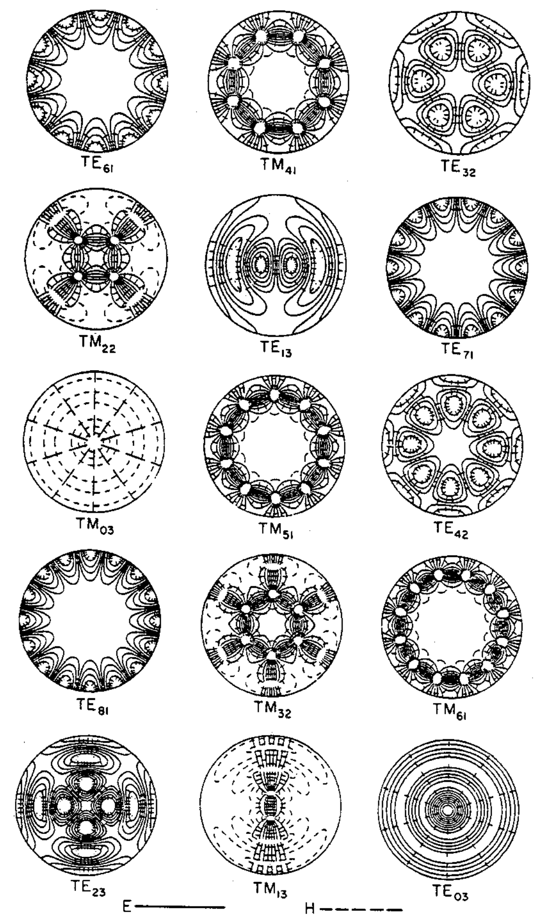

Fig. 6. (*Continued*)

The density of the field lines is approximately proportional to the field strength. These plots are done by a Cyber 175 computer.

References

[1] G. C. Southworth, "Hyper-frequency waveguides—General considerations and experimental results," *Bell Syst. Tech. J.*, vol. 15, pp. 284–309, Apr. 1936.

[2] W. L. Barrow, "Transmission of electromagnetic waves in hollow tubes of metals," *Proc. IRE*, vol. 24, pp. 1298–1328, Oct. 1936.

[3] S. A. Schelkunoff, "Transmission theory of plane electromagnetic waves," *Proc. IRE*, vol. 25, pp. 1457–1493, Nov. 1937

[4] L. J. Chu and W. L. Barrow, "Electromagnetic waves in hollow metal tubes of rectangular cross section," *Proc. IRE*, vol. 26, pp. 1520–1555, Dec. 1937.

Computations of Frequencies and Intrinsic Q Factors of TE_{0nm} Modes of Dielectric Resonators

JERZY KRUPKA

***Abstract*—The Rayleigh–Ritz method is described, which is used to calculate the resonant frequencies and intrinsic Q factors due to dielectric**

Manuscript received August 7, 1984; revised October 29, 1984.

The author is with the Instytut Technologii Elektronowej, Politechnika Warszawska ul. Koszykowa 75, 00-662 Warszawa, Poland.

0018-9480/85/0300-0274$01.00 ©1985 IEEE